XIX IMEKO World Congress
Fundamental and Applied Metrology
September 6–11, 2009, Lisbon, Portugal

HIGH SENSITIVITY TRIAXIAL MAGNETIC FIELD TRANSDUCER, BASED ON THE PHASE CHARACTERISTICS OF THE GMI EFFECT

E. Costa Silva [1], *L. A. P. Gusmão* [2], *C. R. Hall Barbosa* [3], *E. Costa Monteiro* [4]

[1] Post Graduate Program in Metrology / PUC-Rio, Rio de Janeiro, Brazil, eduvasco2002@terra.com.br
[2] Electrical Engineering Department / PUC-Rio, Rio de Janeiro, Brazil, lgusmao@ele.puc-rio.br
[3] Post Graduate Program in Metrology / PUC-Rio, Rio de Janeiro, Brazil, hall@ele.puc-rio.br
[4] Post Graduate Program in Metrology / PUC-Rio, Rio de Janeiro, Brazil, beth@puc-rio.br

Abstract – The Laboratory of Biometrology of PUC-Rio has been developing magnetic field transducers to be used in biomedical applications. Investigations recently accomplished indicate the possibility of a new research line, which considers the changes in the phase characteristics of Giant Magnetoimpedance (GMI) sensors due to varying low-intensity magnetic fields. In spite of being less explored in the literature, the work carried out so far indicates that the sensitivity of the phase can lead to more promising results than the ones already obtained with transducers based on the variation of the impedance magnitude. This manuscript discusses the development process of a new class of magnetic field transducers, beginning with the definition of the ideal stimulation condition for the sensor elements, proceeding to discuss the configuration that makes possible a triaxial measurement and closing with the electronic circuit that conditions the GMI ribbons and reads their phase variation as a function of an axial magnetic field. Simulation studies of a complete transducer, including the conditioning circuit and based on data obtained from measured curves, have shown that an improvement in sensitivity greater than 20 times can be expected when compared to the previous magnitude-based transducers.

Keywords: Biometrology, Giant Magnetoimpedance, Phase, Magnetic Field Transducer.

1. INTRODUCTION

1.1. Historical context

The Post Graduate Program in Metrology of PUC-Rio, through the research line in Biometrology and in partnership with the Department of Physics of the Federal University of Pernambuco (UFPE), has been carrying out studies seeking the implementation of prototypes of magnetometers based on the Giant Magnetoimpedance (GMI) phenomenon [1-3].

The importance of GMI in the world's scientific scenery has been increasing, and several laboratories are accomplishing promising researches in different application areas. A recent example was the 2007 Nobel Award in Physics to the researchers Albert Fert and Peter Grünberg, who discovered the giant magneto-resistance, GMR [4,5].

The GMI effect started to be studied intensely in the 90's. The first results obtained in such studies were interpreted as a variation of the Giant Magnetoresistance effect (GMR), whose experimental behavior is examined with the application of a continuous current and in the presence of a continuous magnetic field.

The GMR effect considers only the variation of the resistance, and the phenomenon is explained by the change in the electrons motion when their spin is affected by the orientation of a magnetization [4]. However, experiments accomplished with samples of amorphous ferromagnetic alloys, using alternating currents, have shown a variation of the resistive component as well as of the reactive component with respect both to the external magnetic field and to the frequency of the applied current. Thence comes the designation GMI.

1.2. GMI effect

This work focuses on a particular case of GMI named Longitudinal Magnetoimpedance (LMI). The LMI phenomenon is induced by the application of an alternating current (I) along the length of a ribbon (or wire), which is submitted to an external magnetic field (H) parallel to it. The difference of potential (V) is then measured between the extremities of the ribbon, as shown in Fig. 1.

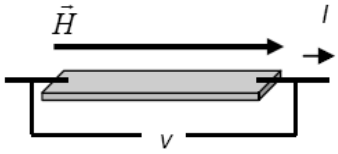

Fig. 1. Typical GMI measurement.

Using the phasorial description of the AC voltage and current, as well as arbitrating the phase of the current (ϕ_I) as zero, the impedance of the sample can be calculated as:

$$Z = \frac{|V|e^{\phi_V}}{|I|e^{\phi_I}} = \frac{|V|}{|I|}e^{\phi} = |Z|\cos\phi + j|Z|\sin\phi = R + jX \quad (1)$$

The GMI effect is actually a result of the skin depth dependency with the magnetic permeability, which varies not only with the external magnetic field that is applied to the sample, but also with the frequency and intensity of the current that passes through it. Then, in agreement with the literature [6-7], it can be stated that:

$$Z=(1-i)\frac{L}{2\omega\sigma\delta}\frac{1}{1-e^{-(1-i)t/2\delta}}\text{ , and} \quad (2)$$

$$\delta=\frac{c}{2\pi}\sqrt{\frac{1}{2\omega\mu\sigma}}\text{ ,} \quad (3)$$

where ***L*** is the length and ***t*** is thickness of the ribbon, ***ω*** is the frequency of the current and ***σ*** is the conductivity of the material.

1.3. AGMI effect

The GMI curves, which indicate the variation of the impedance with the external magnetic field (H), are usually symmetrical in relation to this field. However, it has been noticed that certain conditions favor the emergence of an asymmetry in those curves, denominated Asymmetric Giant Magnetoimpedance, or AGMI effect. In spite of the fact that not all causes of AGMI are well known, three factors are highlighted in the literature: (a) asymmetry due to DC current; (b) asymmetry due to AC magnetic field and (c) asymmetry due to "exchange bias" [8-10].

However, as it will be seen in the subsequent sections, the focus here was to induce the AGMI by overlapping a DC biasing current to the alternating current (AC) used in the GMI measurements. This alone alters significatively the form of the GMI curves in function of the magnetic field.

By means of AGMI, it is possible to improve the magnitude (***d|Z|/dH***) or phase (***dθ/dH***) sensitivity. This asymmetry is characterized by an increase of one of the peaks, or valleys, with a decrease of the other, in either the ***|Z|xH*** or the ***θxH*** curves, as it will be shown in Section 2.2.

1.4. Previous Works

As examples of transducers developed at PUC-Rio, which are based on the magnitude variation of the GMI effect and uses GMI ribbons as sensor elements, it can be mentioned the transducer for localization of needles inserted in the human body shown in Fig. 2 (which sensitivity was 12V/Oe), and the transducer for measurement of arterial pulse waves shown in Fig. 3 (which sensitivity was 1mV/Pa) [1,2].

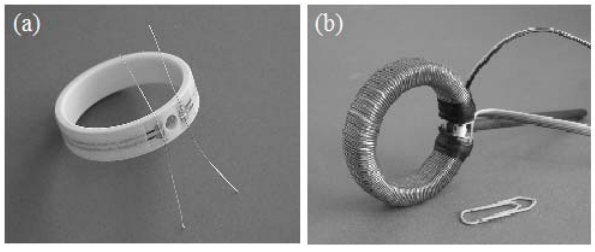

Fig. 2. (a) Partial ring shaped prototype with GMI ribbons fastened; (b) Complete prototype with the excitation coils.

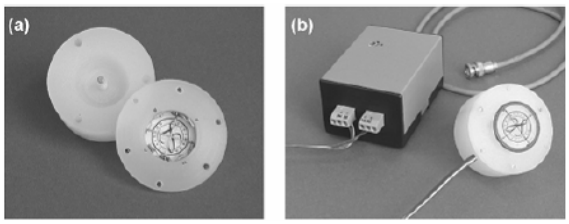

Fig. 3. (a) Opened prototype without the electronic circuit; (b) Complete prototype.

Seeking to improve the transducers sensitivity, the behavior of the impedance phase of the GMI effect was analyzed (instead of the impedance magnitude), as well as the use of the AGMI effect and of structural changes in the configuration of these transducers [3]. This approach has been effective and will be discussed throughout this work.

2. DEVELOPMENT PROCESS

2.1. Methods and Procedures

The GMI ribbons were put in the center of a Helmholtz Coil, as shown in Fig. 4, in order to be excited by a magnetic field longitudinal to the direction of the current that flows through them. Still, the ribbon-coil set was positioned in a way to guarantee that the magnitude of the earth magnetic field was transversal to the ribbons. Thus, its influence in the measurements was minimized (the GMI ribbons used are of the LMI type, characterized by a very low sensitivity to transversal fields).

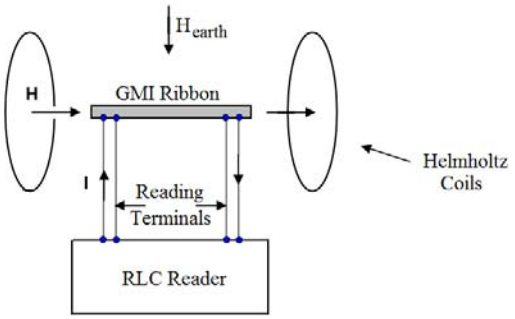

Fig. 4. Blocks Diagram of the system used in the characterization of the GMI ribbons.

The magnitude and phase readings were accomplished by an RLC meter, which was also responsible for both AC and DC stimulation of the ribbons. The variation of the magnetic field generated by the Helmholtz Coil was accomplished by a DC Current Source, according to (4).

$$H=\frac{8\mu_0 NI}{5\sqrt{5}R}\approx 9\times10^{-3}\frac{NI}{R}[Oe] \quad (4)$$

where ***H*** is the magnetic field in the center of the Helmholtz coils, ***N*** the number of coils, ***I*** the current that flows through the coils and ***R*** the radius of the coils.

The Helmholtz Coils have 48 coils and a radius of 15cm, yielding:

$$H[Oe]=2,877\times I[A] \quad (5)$$

It should be highlighted (as depicted in the next subsection figures) that negative field values (H) indicates that the current that flows through the ribbon has the same direction of the field generated by the Helmholtz Coil, and for positive field values the opposite occurs.

2.2. Phase characterization

All the measurements were made in $Co_{70}Fe_5Si_{15}B_{10}$ ribbon-shaped alloys with an average thickness of 60 µm and an average width of 1,5 mm. The AC current amplitude was kept in 15 mA, because it has been previously seen that such parameter did not affect the GMI ribbon behavior significantly. Thus, studies have been accomplished with the described GMI ribbon, analyzing the influence of the excitation current DC level (0 mA to 100 mA) and of the frequency (100 kHz to 10 MHz). Also, it has been investigated how the ribbon length (1 cm, 3 cm, 5 cm and 15 cm) affects the sensitivity and which is the best biasing field.

In spite of having carried out studies of the ribbons magnitude and phase behaviour [3], this work focuses in the phase characteristics, which have presented better results. For the sake of conciseness, only the best results for each of the four different tested lengths are herein presented.

Figs. 5 to 8 present, for several current frequencies and an 80 mA DC current level, the variations of the ribbons impedance phase as a function of the parallel magnetic field. In such figures, θ_0 is the value of the phase in the case of a null external magnetic field parallel to the ribbon length.

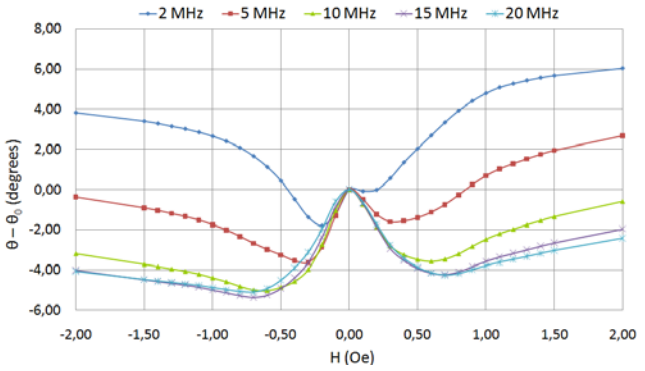

Fig. 5. Phase of the impedance of a 15 cm long GMI ribbon submitted to an 80 mA DC current.

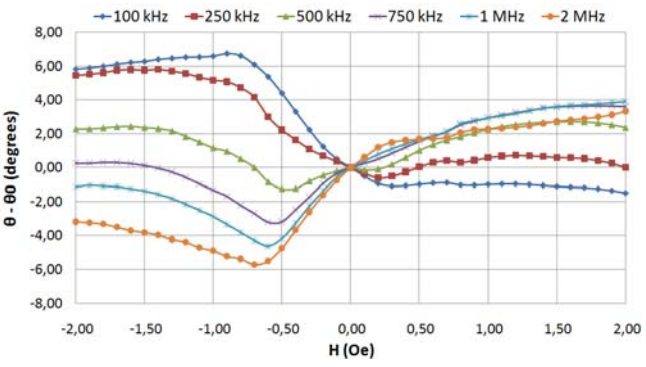

Fig. 6. Phase of the impedance of a 5 cm long GMI ribbon submitted to an 80 mA DC current.

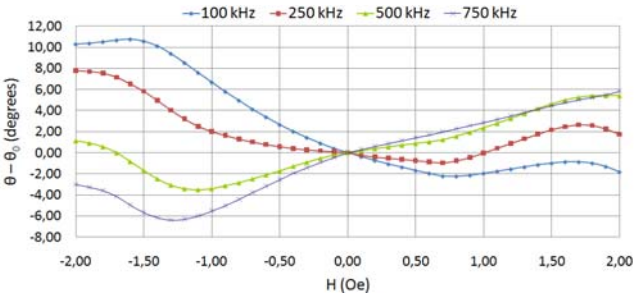

Fig. 7. Phase of the impedance of a 3 cm long GMI ribbon submitted to an 80 mA DC current.

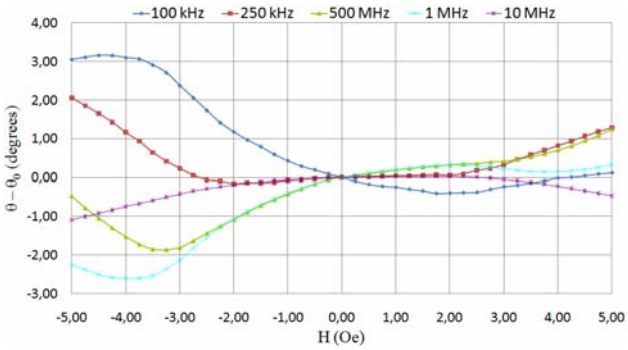

Fig. 8. Phase of the impedance of a 1 cm long GMI ribbon submitted to an 80 mA DC current.

On the other hand, Figs. 9 to 12 show the phase variations for several DC current levels and different frequencies, also in function of the magnetic field parallel to the ribbon.

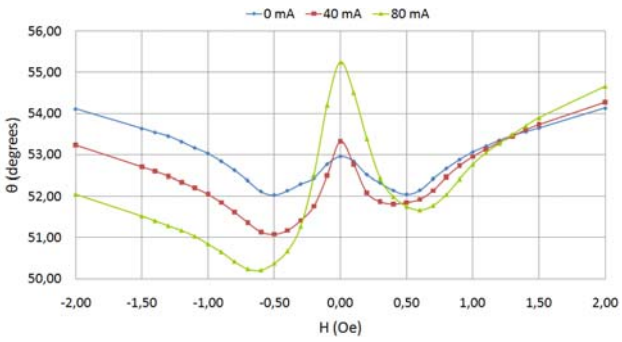

Fig. 9. Phase of the impedance of a 15 cm long GMI ribbon submitted to a 10 MHz current.

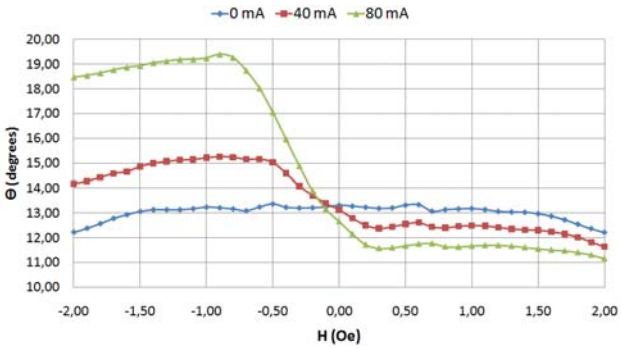

Fig. 10. Phase of the impedance of a 5 cm long GMI ribbon submitted to a 100 kHz current.

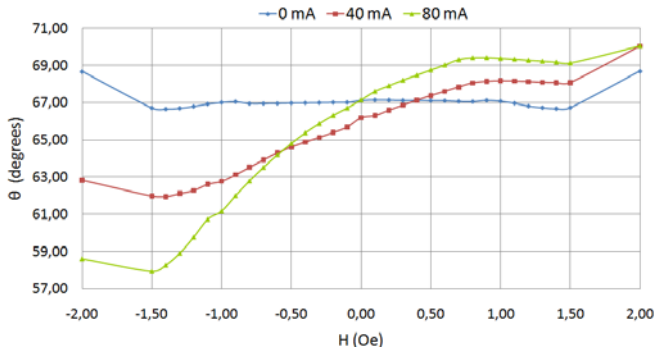

Fig. 11. Phase of the impedance of a 3 cm long GMI ribbon submitted to a 2 MHz current.

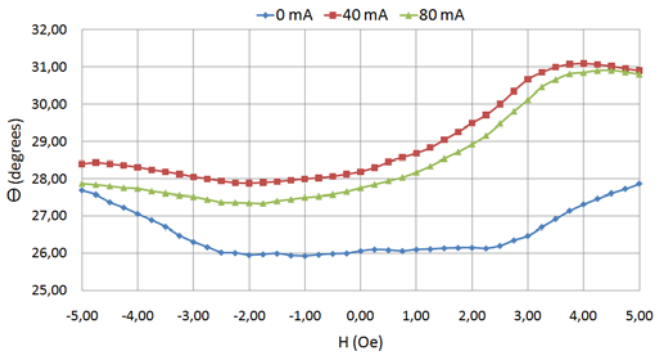

Fig. 12. phase of the impedance of a 1 cm long GMI ribbon submitted to a 100 kHz current.

The presented graphs (Figs. 5 to 12) show that the phase characteristics are affected by all of the analyzed parameters: ribbon length, DC level and frequency. Table 1 presents the GMI ribbons maximum sensitivity, for each one of the tested lengths, and considering only their respective best conditioning situation (i.e., the optimal applied current).

Table 1. Summary of optimal sensitivity by ribbon length.

Ribbon Length (cm)	Applied Current (mA)	Sens. (degrees /Oe)	Equivalent Sensitivity (degrees /Oe)
1	80 + 15 sin (2π100kHz t)	1,3	19,5
3	80 + 15 sin (2π100kHz t)	9,0	45,0
5	80 + 15 sin (2π100kHz t)	10,8	32,4
15	80 + 15 sin (2π10MHz t)	17,0	17,0

The column called "equivalent sensitivity" has been added in table 1 for a fair comparison between the performance of the ribbons with different lengths, relating them with the 15 cm ribbon. This is why, for example, in its first entry the column shows the sensitivity value of the 1cm ribbon multiplied by fifteen.

2.3. Geometric Configuration

Based on the fact the GMI ribbons of the LMI type are sensitive only to the magnetic field component parallel to their length, it has been idealized a configuration that allows the triaxial reading of an external magnetic field.

Fig. 13 illustrates the envisaged topology, which uses, in each axis, a GMI ribbon. The configuration also allows for an only and common origin of the coordinates system.

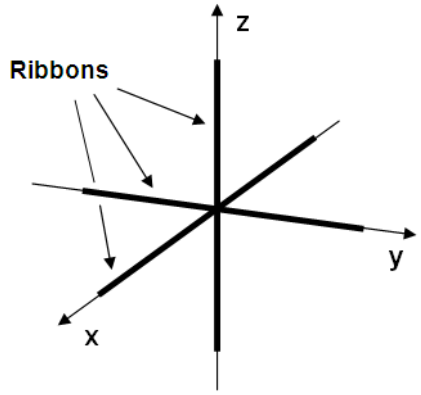

Fig. 13. Sensor elements triaxial configuration.

The biasing magnetic field, which is necessary to make the ribbons to operate in their most sensitive region, can be applied by a single solenoidal winding encircling the three ribbons. To this end, the solenoid axis should be sloped regarding to all ribbons, as illustrated in Fig. 14. It can be easily shown that $\theta = 35{,}26^{o}$ allows for

$$H_x = H_y = H_z = 0{,}577 H_{sol} \qquad (6)$$

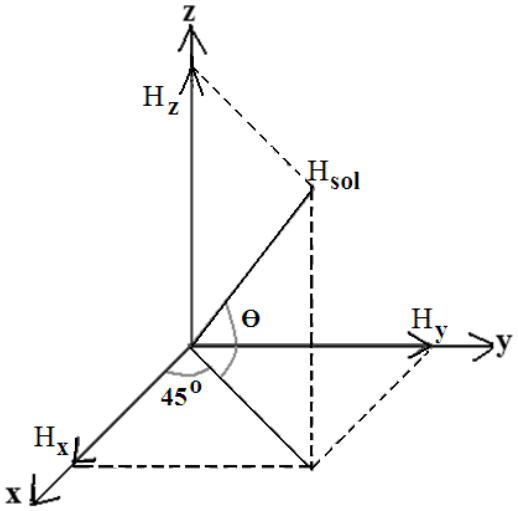

Fig. 14. Solenoid magnetic field (H_{sol}) and the ribbons polarization magnetic fields (H_X, H_Y, H_Z).

The magnetic field in a solenoid (H_{sol}) is directly proportional to a DC current, according to

$$H_{sol}[Oe] = 10^4 B_{sol}[T] = \frac{10^4 \mu N i}{L} \qquad (7)$$

where $\boldsymbol{\mu}$ is the magnetic permeability, $\boldsymbol{N}$ is the number of coils, $\boldsymbol{i}$ is the current and $\boldsymbol{L}$ is the solenoid length.

As the components H_X, H_Y, H_Z are identical, the optimum polarization field of all the ribbons can be easily set by adjusting the current that flows through the solenoid.

2.4. Electronic Circuit

The block diagram of the proposed phase detection and conditioning circuit, to be used in the implementation of the new transducer, is presented in Fig. 15.

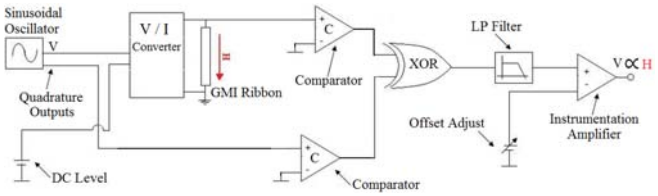

Fig. 15: Conditioning and phase reading electronic circuit.

The idealized circuit is capable of conditioning the ribbon, supplying the AC current (with the appropriate frequency and amplitude) and the specified DC level. It also delivers a voltage output which is proportional to the phase variation of the ribbons impedance ($\Delta\theta$).

3. SIMULATED RESULTS

Based on the experimental results obtained from their phase characterization (Section 2.2), the ribbons were electrically modelled in order to simulate the transducer behaviour. The modelling approach consisted, basically, in applying to equation (1) the obtained experimental data. Hence, all ribbons were modelled as a resistive component in series with an inductance [3].

Then, the sensitivity of the transducer – comprising the GMI ribbons and the electronic circuit – has been evaluated by means of a SPICE program. For an excitation current with 80mA DC level, 15 mA AC amplitude and 100 kHz applied to a 3 cm ribbon, the results indicate a sensitivity of 275 V/Oe.

4. CONCLUSIONS

The results show that, by exploring the phase characteristics of GMI ribbons, it is possible to obtain good sensitivities with low excitation frequencies, thus facilitating the implementation of the transducer electronic circuit. Still, it must be pointed out that the simulated sensitivity of the envisaged transducer is 23 times better than the sensitivity presented by the previous prototype (based on the impedance magnitude), even using GMI ribbons with a much smaller overall length (3 cm versus 30 cm).

Besides the above mentioned aspects, the newly idealized transducer introduces a key feature, not existent in the previous prototypes, that allows the triaxial reading of the magnetic field to be measured.

As it can be also noted, the developed equipment tries to comply with the Biometrological Principles, which request high accuracy, non-invasivity, innocuity, low cost of production and operation, besides a low operation complexity [11].

To conclude, it must be said that the goal of our research group is to continue the improvements in the new transducer, seeking its use in the detection of non-magnetic metallic bodies inserted in the human body and, in a more ambitious task, in the detection of very weak biological signals as, for example, those generated by the human heart (in the order of 10^{-11} T).

ACKNOWLEDGMENTS

We would like to thank CNPQ and FINEP for the support and supplied resources. Still, we would like to express our gratitude to Professor Fernando Luis de Araújo Machado of the Physics Department of UFPE for the cooperation and continuous knowledge exchange.

REFERENCES

[1] F. Pompéia, L. A. P. Gusmão, C. R. Hall Barbosa, E. Costa Monteiro, L. A. P. Gonçalves, F. L. A. Machado, "Ring shaped magnetic field transducer based on the GMI effect", Meas. Sci. Technol., http://www.iop.org/EJ/abstract/0957-0233/19/2/025801/ DOI 10.1088/0957-0233/19/2/025801, January 2008.

[2] D. Ramos Louzada, E. Costa Monteiro, L. A. P. Gusmão, C. R. Hall Barbosa, "Arterial pulse waves non-invasive measurement using a GMI pressure transducer", "Medição não-invasiva de ondas de pulso arterial utilizando transdutor de pressão MIG", Proceedings of the IV Latin American Congress on Biomedical Engineering, Brazil, Sept. 2007

[3] E. Costa Silva, L. A. P. Gusmão, C. R. Hall Barbosa, E. Costa Monteiro, "Magnetic Field Transducers based on the Phase Characteristics of GMI Sensors and Aimed to Biomedical Applications", Proceedings of the 13th International Conference on Biomedical Engineering, ICBME2008, Singapore, December 2008.

[4] A. Fert, "The origin, development and future of spintronics", Nobel Lecture, at http://nobelprize.org/nobel_prizes/physics/laureates/2007/fert_lecture.pdf, Stockholm, Sweden, 2007.

[5] P. Grünberg "From spinwaves to giant magneto magnetoresistence (GMR) and beyond", Nobel Lecture, at http://nobelprize.org/nobel_prizes/physics/laureates/2007/grunberg_lecture.pdf, Stockholm, Sweden, 2007.

[6] F. L. A. Machado and S. M. Rezende, "A theoretical model for the giant magnetoimpedance in ribbons of amorphous soft-ferromagnetic alloys", J. Appl. Phis., vol. 79, pp. 6958–6960, DOI 10.1063/1.361945, 1996.

[7] V. Knobel and K. R. Pirota, "Giant magnetoimpedance concepts and recent progress", J. Magn. Magn. Mater., vol. 242, pp. 33–40, DOI 10.1016/S0304-8853(01)01180-5, 2002.

[8] F. L. A. Machado, A. R. Rodrigues, A. A. Puça, A. E. P. de Araújo, "Highly Asymmetric Giant Magnetoimpedance", *Materials Science Forum*, vol. 302-303, p. 202-208, 1999.

[9] C. G. Kim, K. J. Jang, H. C. Kim, S. S. Yoon, "Asymmetric giant magnetoimpedance in field-annealing Co-based amorphous ribbon", *Journal of Applied Physics*, vol. 85, p. 5447- 5449, 1999.

[10] D. P. Makhnovskiy, L. V. Panina, D. J. Mapps, "Asymmetric Magnetoimpedance in as-cast CoFeSiB Amorphous Wires due to ac Bias.", *Applied Physics Letter*s, vol. 77, p. 121-123, 2000.

[11] E. Costa Monteiro, "Biometrology: Reliability in Biomeasurements and Ethical Repercussions", "Biometrologia: Confiabilidade nas Biomedições e Repercussões Éticas", Metrologia e Instrumentação, v. 6, p. 6-12, Brazil, 2007.